Osteoarthritis and Cartilage 18 (2010) 1509–1517

Osteoarthritis and Cartilage

OARSI OSTEOARTHRITIS RESEARCH SOCIETY INTERNATIONAL

Mechanical impact induces cartilage degradation *via* mitogen activated protein kinases

L. Ding †, E. Heying ‡, N. Nicholson †, N.J. Stroud §, G.A. Homandberg ||, J.A. Buckwalter †¶, D. Guo ||, J.A. Martin †*

† *Department of Orthopaedics and Rehabilitation, University of Iowa Hospitals and Clinics, Iowa City, Iowa, USA*
‡ *Department of Biology, Wartburg College, Waverly, Iowa, USA*
§ *Department of Biomedical Engineering, University of Iowa, Iowa City, Iowa, USA*
|| *Department of Biochemistry and Molecular Biology, University of North Dakota, Grand Forks, North Dakota, USA*
¶ *Veterans Affairs Medical Center, Iowa City, Iowa, USA*

ARTICLE INFO

Article history:
Received 8 December 2009
Accepted 19 August 2010

Keywords:
Impact
Cartilage damage
MAP kinases
Inhibitors
Post-traumatic osteoarthritis

SUMMARY

Objective: To determine the activation of Mitogen activated protein (MAP) kinases in and around cartilage subjected to mechanical damage and to determine the effects of their inhibitors on impaction-induced chondrocyte death and cartilage degeneration.
Design: The phosphorylation of MAP kinases was examined with confocal microscopy and immunoblotting. The effects of MAP kinase inhibitors on impaction-induced chondrocyte death and proteoglycan (PG) loss were determined with fluorescent microscopy and 1, 9-Dimethyl-Methylene Blue (DMMB) assay. The expression of catabolic genes at mRNA levels was examined with quantitative real-time PCR.
Results: Early p38 activation was detected at 20 min and 1 h post-impaction. At 24 h, enhanced phosphorylation of p38 and extracellular signal-regulated protein kinase (ERK)1/2 was visualized in chondrocytes from in and around impact sites. The phosphorylation of p38 was increased by 3.0-fold in impact sites and 3.3-fold in adjacent cartilage. The phosphorylation of ERK-1 was increased by 5.8-fold in impact zone and 5.4-fold in adjacent cartilage; the phosphorylation of ERK-2 increased by 4.0-fold in impacted zone and 3.6-fold in adjacent cartilage. Furthermore, the blocking of p38 pathway did not inhibit impaction-induced ERK activation. The inhibition of p38 or ERK pathway significantly reduced injury-related chondrocyte death and PG losses. Quantitative Real-time PCR analysis revealed that blunt impaction significantly up-regulated matrix metalloproteinase (MMP)-13, Tumor necrosis factor (TNF)-α, and ADAMTS-5 expression.
Conclusion: These findings implicate p38 and ERK mitogen activated protein kinases (MAPKs) in the post-injury spread of cartilage degeneration and suggest that the risk of post-traumatic osteoarthritis (PTOA) following joint trauma could be decreased by blocking their activities, which might be involved in up-regulating expressions of MMP-13, ADAMTS-5, and TNF-α.

Introduction

Joint injury is a common cause of osteoarthritis (OA) in young adults and is responsible for about 12% of all OA of the lower extremity joints[1–3]. In this disorder the initial cartilage lesion is caused by direct mechanical force. Examination of injured cartilage shows loss of proteoglycan (PG) from the extracellular matrix (ECM) and disruption of collagen fiber network[4,5]. More recent findings showed that chondrocyte density is progressively decreased following blunt impact[6–8]. The reduction of cellularity is correlated with the severity of post-traumatic osteoarthritis (PTOA)[9]. Cell death initiated by mechanical trauma has been observed both *in vivo* and *in vitro*[10–13]. The mechanisms involved in this type of trauma-induced cell death include necrosis[14], chondropotosis (a variant of apoptosis in chondrocytes)[15], and apoptosis[16–19]. While the direct impact causes necrosis of chondrocytes, the spreading of cell death into adjacent cartilage is most likely induced by apoptosis/chondropotosis which is a highly regulated process carried out by intracellular signaling cascades.

Mitogen activated protein (MAP) kinases, p38, extracellular signal-regulated kinases (ERKs), and c-Jun N-terminal kinases

* Address correspondence and reprint requests to: James A. Martin, Department of Orthopaedics and Rehabilitation, University of Iowa Hospitals and Clinics, 500 Newton Road, 1182 Medical Laboratories, Iowa City, Iowa 52242, USA.
E-mail address: james-martin@uiowa.edu (J.A. Martin).

1063-4584/$ – see front matter © 2010 Osteoarthritis Research Society International. Published by Elsevier Ltd. All rights reserved.
doi:10.1016/j.joca.2010.08.014

(JNKs), are implicated in mediating cartilage damage by up-regulating matrix metalloproteinases (MMPs)[20] that degrade the ECM. The activation of MAP kinases has been observed in various osteoarthritic-cartilage-damage models, such as IL-1beta induced chondrolysis[21] and cartilage damage induced by matrix degradation products including fibronectin fragments[22] and collagen fragments[23,24]. Furthermore, MAP kinases also play essential roles in apoptotic pathways. In Hela cells, p38 MAP kinase was activated in response to apoptotic signals initiated by the depletion of Cdc7, a key kinase involved in DNA replication and checkpoint response[25]. The death of a human Leukemia cell line, HL-60, induced by diallyl disulfide (DADS) was mediated by the activation of p38 MAP kinase while the activity of another MAP kinase, ERK, was inhibited[26]. Similar results were observed in another Leukemia cell line, U937, when treated with phospholipase A_2[27]. However, when human gastric cells were treated with hydrogen peroxide, both ERK and JNK MAP kinases were activated, resulting in apoptosis[28]. Furthermore, in an experimental OA animal model created with sectioning of the anterior crucial ligament, the activation of MEK1/2, the upstream kinase of ERK1/2, and p38 MAP kinase was demonstrated to be responsible for the up-regulation of iNOS and COX-2 which mediate chondrocyte apoptosis[29].

Because of their involvement in cartilage damage/chondrolysis pathways, we hypothesized that MAP kinases, especially ERK and p38, activated in response to a single blunt impact injury contribute to chondrocyte death and PG loss in and around the impact site. To test this we used an osteo-chondral explant model to study the time course of MAP kinase activation and to study the effects of specific inhibitors on impact-related chondrocyte death and PG losses in impacted and surrounding cartilage.

Methods

All common chemicals and reagents were purchased from RPI Corp. (Mount Prospect, IL) or Sigma Chemical Co. (St. Louis, MO). Dulbecco's Modified Eagle Medium (DMEM), F-12, Fetal Bovine Serum (FBS), and Hanks' Balanced Salt Solution (HBSS) were from Gibco/Invitrogen (Carlsbad, CA). Methanol-free 16% paraformaldehyde solution was purchased from Thermo Fisher Scientific (Rockford, IL). Goat serum was from Sigma–Aldrich® (St. Louis, MO). Alexa Fluor® 568 F(ab′)2 fragment of goat anti-rabbit IgG (H + L) was obtained from Invitrogen™ (Carlsbad, CA). VECTASHIELD mounting medium with DAPI was from Vector Laboratories, Inc. (Burlingame, CA). Protease inhibitor cocktail set III reagent was purchased from Calbiochem/EMD (Gibbstown, NJ). Bicinchoninic Acid (BCA) Protein Assay Reagent was from Thermo Scientific/Pierce Biotechnology (Rockford, IL). Total and phosphor-specific p38 (Thr180/Tyr182), JNK1/2 (Thr183/Tyr185), ERK1/2 (Thr202/Tyr204) antibodies and horse radish peroxidase (HRP)-conjugated goat anti-rabbit IgG were from Cell Signaling Technology (Danvers, MA). The chemical inhibitors of p38 MAP kinase, SB203580 and SB202190, and inhibitors of MEK1/2/ERK1/2, and U0126 were purchased from CalBiochem® (San Diego, CA). Dimethyl Sulfoxide (DMSO) (molecular biology grade, ≥99.9%), 1, 9-Dimethyl-Methylene Blue (DMMB), and papain were obtained from Sigma–Aldrich (St. Louis, MO). Calcein AM and ethidium homodimer-2 (EthD-2) were from Invitrogen™ (Carlsbad, CA). Pure Nitrocellulose Membranes (0.45 μM) were purchased from Bio-Rad Laboratories (Hercules, CA). SuperSignal West Dura Extended Duration Substrate was from Thermo Scientific/Pierce Biotechnology (Rockford, IL). BioMax XAR Film was purchased from Kodak Film (Rochester, NY). Biopsy punches were from Miltex (York, PA).

Stifle joints were taken from 18 to 20-month-old cows from a local abattoir. 2.5 cm × 2.5 cm (W × L) osteo-chondral explants with 0.5–1.0 cm-thick subchondral bone were manually sawed from the central loaded area of the lateral tibial plateau. The explants were then washed once with 1× HBSS containing antibiotics, placed in culture media [DMEM/F-12 (50%/50%)/10% FBS, with antibiotics] and incubated overnight at 37°C (5% CO_2, and 5% O_2).

A drop tower was employed to impart loads to an indenter resting on the cartilage surface of the explants. The indenter was a flat-faced 5.0 mm diameter brass rod with rounded edges ($r = 1$ mm). A 2 kg mass was dropped onto the rod from a height of 14 cm resulting in impact energy density of 14 J/cm^2. Impacted explants were placed in fresh culture media and incubated at 37°C, 5% CO_2, and 5% O_2 for various times. Impact sites were visible to the naked eye immediately after insult [Fig. 1(A)]. Safranin-O histology revealed local delamination and superficial/transitional zone fissuring typical of high energy blunt impact injuries [Fig. 1(C)].

In order to visualize the distribution of phosphorylated kinases, cartilage from explants at 24 h post-impaction or from non-impacted explants at the corresponding time point was embedded in Tissue Freezing Medium (Triangle Biomedical Sciences, Durham, NC) and full-thickness sagittal sections were cut at 5 μm–10 μm intervals. The sections were fixed with 4% paraformaldehyde for 15 min at room temperature (RT), washed three times with 1× PBS, and blocked for 1 h at RT with 5% goat serum diluted in 1× PBS containing 0.3% Triton X-100. After blocking, sections were incubated overnight at 4°C with anti-phospho p38 antibody or anti-phospho-ERK1/2 antibody diluted 1:100 in 1% BSA/PBS containing 0.3% Triton X-100. After three washes, sections were incubated with Alexa 568 conjugated goat anti-rabbit IgG diluted 1:400 in 1% BSA/PBS containing 0.3% Triton X-100 for 1–2 h at RT. After final washes with 1× PBS, sections were mounted in VECTASHIELD/DAPI mounting medium. Alexa 568 fluorescence representing phosphorylated MAP kinases and DAPI fluorescence representing cell nuclei were imaged with a Zeiss 710 confocal microscope.

Cartilage for phosphoprotein analysis was harvested at 20 min, 1 h, 3 h, 6 h, 12 h, 24 h, and 48 h post-impact. Non-impacted control cartilage was harvested at the same time points. 6 and 8 mm diameter biopsy punches and an osteotome were used to separate the impacted and annulus cartilage from the bone [Fig. 1(B)]. Impacted and annulus cartilage, both cut in half with scalpels, were immediately submerged into cold lysis buffer (150 mM NaCl, 10 mM Tris, pH 7.0, 0.1% SDS, 1% Triton X-100, 1% sodium deoxycholate, 1 mM EGTA, 50 mM NaF, 1 mM Na_3VO_4, 1 mM glycerol phosphate, 2.5 mM sodium pyrophosphate, 10 μg/ml aprotinin, 10 μg/ml leupeptin, 1 mM EDTA). Protease inhibitor cocktail set III was diluted in lysis buffer (1:100). The tissue was incubated in lysis buffer with gentle shaking at 4°C overnight.

After incubation with lysis buffer, supernatants were removed and total protein concentration was determined using the BCA protein assay reagent. Cartilage tissue lysates were denatured with 2× sample buffer and reduced with 0.05 M DTT prior to electrophoresis. Lysate volumes containing 5 μg protein were fractionated on 10% acrylamide SDS gels and electrolotted to nitrocellulose membranes. The blots were blocked with 5% nonfat dry milk in 20 mM Tris buffer, pH 7.4, containing 140 mM NaCl (TBS) and 0.1% Tween 20 (TBST) for 1 h at RT and incubated overnight at 4°C with the anti-total or anti-phospho-specific kinase antibodies diluted 1:1,000 in 5% BSA in TBST (BSA/TBST). This was followed by washing and reaction for 1 h with HRP conjugated goat anti-rabbit IgG diluted 1:2,000 in 5% BSA/TBST. After washing, the blots were reacted with SuperSignal West Dura substrate for 5 min. Blots were then exposed to KODAK BioMax XAR film. Image J software was employed to measure the integrated density (ID) of each band on a blot. The relative fold increase of ID over controls was calculated as: $ID_{pMAPK\ (impaction)}$ X $ID_{\ tMAPK\ (control)}$/[$ID_{pMAPK\ (control)}$ X $ID_{\ tMAPK\ (impaction)}$]. The means and 95% confidence intervals (CI) of the

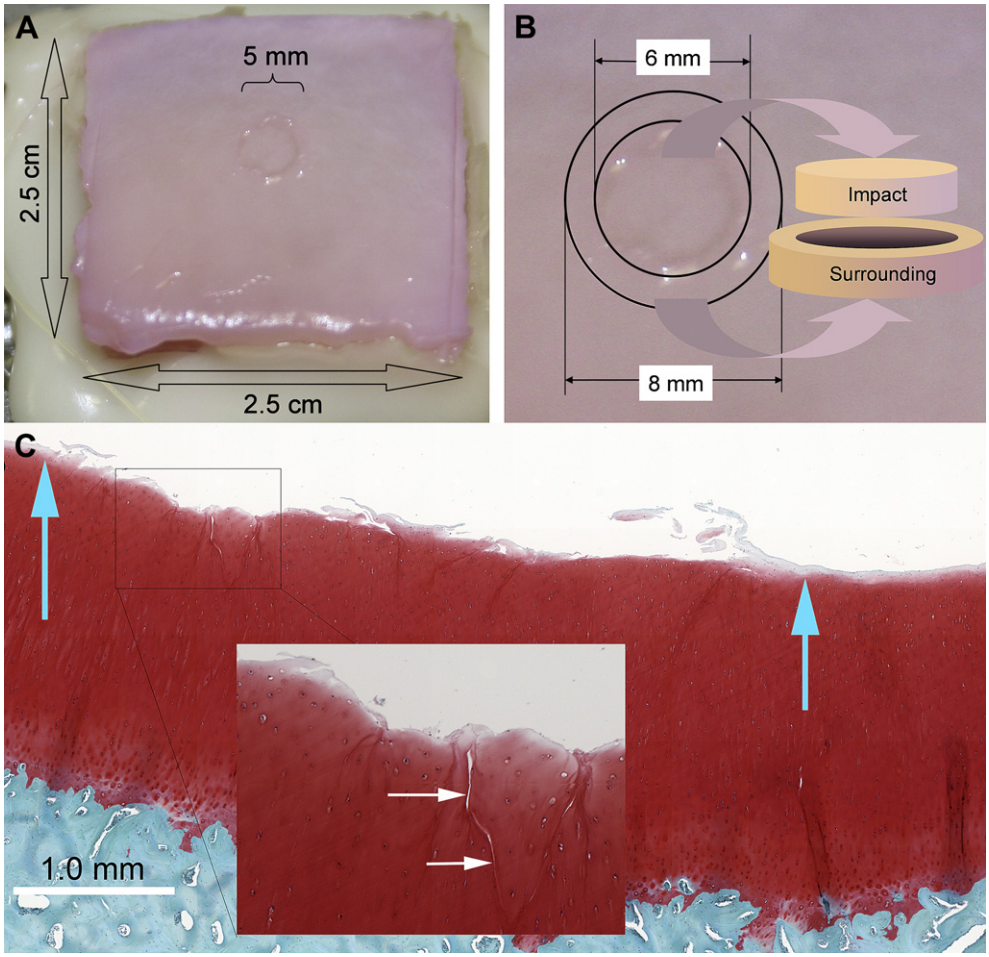

Fig. 1. Osteo-chondral explant blunt injury model. (A) The image shows the gross appearance of a 14 J/cm^2 blunt impact injury on the surface of a typical osteo-chondral explant. The center of the 2.5 cm × 2.5 cm explant was struck once with a 5-mm diameter platen. (B) Illustration of the method employed to harvest cartilage tissue from a traumatized explant. 6 mm punches were used to harvest the impact site itself and 8 mm punches were used to harvest an adjacent annular ring of cartilage surrounding the impact site. (C) A high resolution scanned image of a safranin-O-, fast green-, and hematoxylin-stained section through the middle of an impact site. Blue arrows show the approximate boundaries of the platen contact. The surface is undamaged outside the contact area, but cartilage damage as superficial delamination and cracking are apparent within the impact site. The inset shows a close-up view of cracks running from the surface down to the transitional zone.

relative fold increase were calculated and plotted from at least three individual experiments.

A p38 inhibitor (SB202190) and an ERK inhibitor (U0126) were tested to determine if blocking the p38 pathway inhibits impact-induced ERK activation. Prior to impaction, osteo-chondral explants were pre-treated with either 10 μM SB202190 or 10 μM U0126 for 90 min. After 24 h of post-impaction, cartilage discs were dissected from the impact zone and area surrounding the zone with 6-mm and 8-mm biopsy punches. Cartilage discs from non-impacted explants or from impacted explants without inhibitor pre-treatment were also collected at the same time point. Blots of cartilage lysates were probed with anti-total or − phospho-ERK1/2 antibody as described above.

Two p38 inhibitors (SB203580, SB202190) and an ERK inhibitor (U0126) were tested for effects on impact-induced changes in viability and PG content. All three inhibitors were used at a concentration of 10 μM. Controls were incubated with equivalent volumes of solvent (DMSO), which was 0.1% in culture media. Explants were incubated in mitogen activated protein kinases (MAPK) inhibitors starting 90 min prior to impaction and were returned to culture media containing the inhibitors immediately after impaction. The media were changed and the inhibitors were re-applied every other day. On day 7 post-impact chondrocyte viability in the impact and annulus sites was evaluated by confocal microscopy. Briefly, Osteo-chondral explants were incubated with 1.0 μg/ml calcein AM (live cell staining) and 1 μM ethidium homodimer (dead cell staining) for 45 min, and then washed with 1× HBSS once. Z-section images at 20 μm intervals were taken from three different sites in impacted zone and three in the area surrounding the impacted zone, respectively. Live and dead cells were counted with Image J. The ratio of live cell count to total cell count (chondrocyte viability) was calculated and averaged among three individual experiments. Variances are reported in terms of 95% CIs. Effects were analyzed using one-way ANOVA and the Dunnett test.

The effects of p38 and ERK inhibitors on impact-induced PG loss were examined with DMMB assays. On day 7 post-impact cartilage samples from impact sites were dissected with a 4-mm biopsy punch and osteotome. Five or six cartilage disks in the area immediately next to the impact site were also recovered with 4-mm biopsy punches. The mass of the harvested cartilage disks was measured to obtain wet weight and the cartilage was incubated in papain digest buffer containing 0.5 mg/ml papain, 5 mM L-cysteine, 0.1 M $HNaPO_4$ (pH 7.5) for 4 h at 65 °C. The total sulfated glycosaminoglycan (PG) concentration in the papain digest was measured using DMMB reagent with shark chondroitin sulfate as a standard.

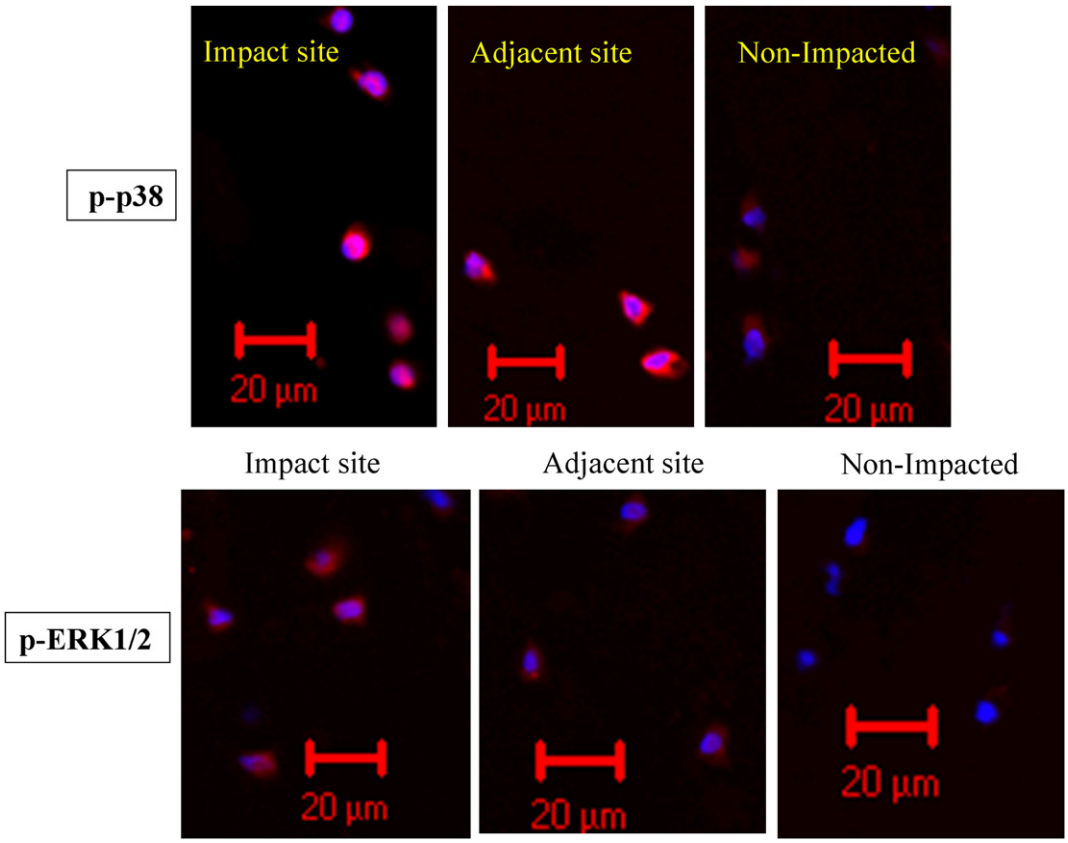

Fig. 2. Effect of blunt impact on enhancing phosphorylation of p38 and ERK MAP kinases. Osteo-chondral explants were pre-equilibrated overnight in DMEM/F12/10% FBS prior to blunt impaction. Cartilage surfaces were subjected to a single blow with an energy of 14 J/cm^2. After 24 h, cartilage discs from the impacted zone and area immediately next to the zone were harvested with 5-mm biopsy punches. Right after harvesting, those discs were immersed into liquid nitrogen for at least 10 min before being transferred into −80°C freezer for storage. Full-thickness of cartilage discs were sectioned at 5 μm or 10 μm intervals. Cartilage sections were immediately fixed with 4% paraformaldehyde. Anti-phospho p38 or anti-phospho-ERK1/2 antibody and Alexa Fluor 568 conjugated goat anti-rabbit antibody were used for indirectly staining of phosphorylated p38 or ERK MAP kinases in chondrocytes. Those sections were counter-stained with DAPI. A Zeiss 710 confocal microscope was utilized to image the distribution of phosphorylated p38 or ERK1/2 MAP kinases.

The amount of PG was normalized to the wet weight of each cartilage disk and was averaged among three individual experiments. Uncertainty estimates are reported as 95% CIs. One-way ANOVA and Holmes–Sidak test was employed for statistical analysis.

MMP-13, Tumor necrosis factor (TNF)-α, and ADAMTS-5 expression was examined at the mRNA level with quantitative real-time PCR (qRT-PCR). Dermal punches were used to dissect impacted, annulus, and control cartilage from four different explants. The cartilage discs were flash frozen in liquid nitrogen and cryosectioned. Total RNA was extracted using TRIZOL® (Invitrogen) and was purified using Qiagen RNEasy Kits (Valencia, CA). The concentration was measured with a Nanodrop spectrometer. Sample volumes containing 50 ng total RNA were assayed by qRT-PCR using Superscript III Platinum SYBR Green One-Step qRT-PCR kits (Invitrogen). Primers for bovine β-actin, MMP-13, TNF-α, and ADAMTS-5 were obtained from Integrated DNA Technologies (Coralville, IA) (sequences available upon request). Data were obtained using an ABI Prism 7700 Sequence detection System (Applied Biosystems, Foster City, CA). Relative gene expression (Impact or Annulus/Control) was calculated using a comparative CT method. Results are reported as fold differences ($2^{-\Delta\Delta CT}$). Treatment effects (impact vs annulus vs control) were evaluated using one-way ANOVA and the Holmes–Sidak test.

Results

Immunofluorescence staining revealed that phosphorylation of p38 MAP kinase in the impact zone was greatly increased compared to non-impacted cartilage at 24 h after impaction (Fig. 2). The phosphorylation level of p38 in cells from cartilage adjacent to the impact zone was also higher than that in non-impacted controls. However, the level of p38 phosphorylation in adjacent

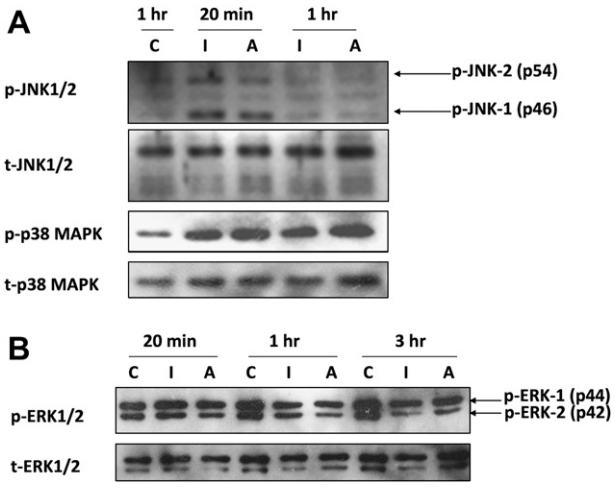

Fig. 3. Short-term Effects of Blunt Impact on MAP kinases. Western blots show results for cartilage from non-impacted control explants ("C") or from impact sites ("I") and annulus sites ("A") from injured explants. The samples were harvested at 20 min, 1 h, and 3 h post-impact or at equivalent culture times in controls. Blots were probed with antibodies recognizing total (t−) and phosphorylated (p−) forms of JNK1/2 and p38 (A) and ERK1/2 (B).

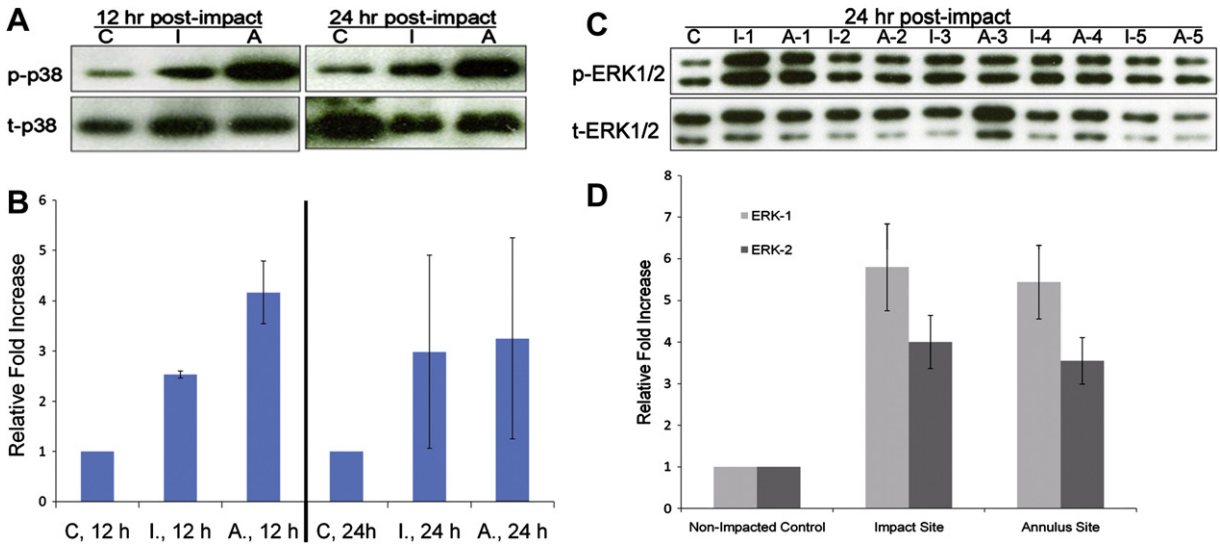

Fig. 4. p38 and ERK MAP Kinase Activation at 12 and 24 h post-impact. Western blot results are shown for cartilage from non-impacted control explants ("C"), or from impact sites ("I") and annulus sites ("A") from injured explants. (A) Representative blots of extracts from cartilage harvested at 12 or 24 h after impact. The blots were probed for total p38 or phosphorylated p38. (B) Fold increase in phosphorylation (impact or annulus vs control) based on densitometric analysis of Western blots from at least three individual experiments. Error bars stand for 95% CIs. (C) Western blots were probed for total and phosphorylated ERKs at 24 h in untreated control or impacted cartilage from five individual osteochondral explants. Results are shown for control, impact and annulus sits ("C", "I", "A"). (D) Average fold increase in phosphorylation (relative to non-impacted control) based on densitometric analysis from six individual experiments. Error bars show 95% CIs.

cartilage was still lower than that in the impact zone. Furthermore, most of phosphorylated p38 was concentrated in the nuclear or peri-nuclear area. Similar to p38, ERK phosphorylation was also enhanced by blunt impact on cartilage, not only in the impact zone but also in the adjacent area.

Immunoblots showed elevated phosphorylation of JNK-1 (p46) and JNK-2 (p54) in both the impact and annulus cartilage at 20 min post-impaction. However, the enhanced phosphorylation declined to baseline at 1 h post-impaction. The activation of p38 MAP kinase was also detected at 20 min post-impaction: phosphorylation in the impacted zone and annulus increased by 2.7- fold and 3.6-fold, respectively. At 1 h post-impaction p38 phosphorylation levels increased to 3.5- and 6.8-fold greater than control in the impact site and annulus respectively [Fig. 3(A)]. In contrast, ERK1/2 activation was not detected within 3 h of post-impaction [Fig. 3(B)].

The activation of p38 MAP kinase was apparent in impacted and annulus cartilage at 12 h post-impaction and was still detectable at 24 h after impact [Fig. 4(A)]. Densitometric analysis of blots from three different experiments showed that at 12 h post-impaction compared to non-impacted controls, the phosphorylation in impacted cartilage was increased by 2.5 ± 0.07-fold and in adjacent cartilage by 4.2 ± 0.62 fold, respectively. At 24 h post-impaction, the phosphorylation levels were still 3.0 ± 1.92 fold higher in impact sites and 3.3 ± 2.00-fold higher in annulus sites when compared to non-impacted controls [Fig. 4(B)].

The activation of ERKs was still undetectable in either the impacted or annulus zones at 12 h after impaction (data not shown). However, at 24 h post-impaction, the phosphorylation of both ERK-1 and -2 was greatly elevated in impacted and annulus cartilage [Fig. 4(C)]. Data from six individual experiments showed the average fold increase of ERK-1 phosphorylation in the impacted zone was 5.8 ± 1.04 and 5.4 ± 0.88 in cartilage surrounding the impacted zone. The phosphorylation of ERK-2 was increased by 4.0 ± 0.64-fold in impacted zone and by 3.6 ± 0.56-fold in annulus cartilage [Fig. 4(D)], Neither JNKs was activated in impacted or annulus cartilage at 12 h or 24 h of post-impaction (data not shown).

Since p38 activation occurred much earlier than ERK1/2 did, the interrelationship of p38 pathway and ERK pathway was also examined. The p38 pathway specific inhibitor, SB202190, did not inhibit the activation of ERK1/2 at 24 h post-impaction (Fig. 5). On the other hand, impaction-induced ERK1/2 phosphorylation was reduced to basal levels by the MEK1/2/ERK1/2 inhibitor, U0126.

Treatment with specific MAP kinase inhibitors greatly enhanced cell viability of impacted explants. Representative images show the cell-sparing effects of the p38 MAPK inhibitor SB202190 [Fig. 6(A)].

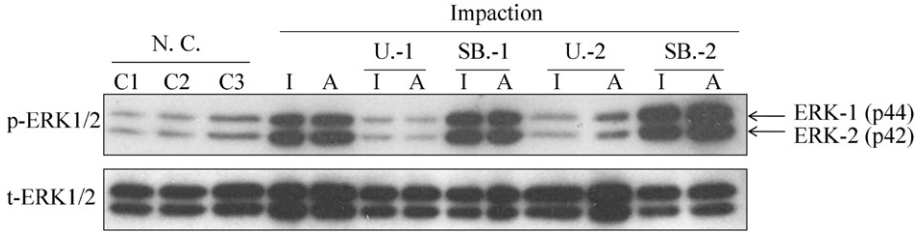

Fig. 5. Effect of blocking p38 MAP kinase activation on blunt impact-induced ERK activation. At 24 h post-impaction, tissue lysates from non-impacted controls (N. C.), from impacted (I) or annulus (A) cartilage. Experimental groups included control explants without any inhibitor treatments, and explants pre-treated with U0126 (U.), a MEK1/2/ERK1/2 inhibitor, or with SB202190 (SB.), a p38 MAP kinase pathway inhibitor. Lysate proteins were resolved by SDS-PAGE and blotted onto nitrocellulose membranes. The membranes were probed with anti-total ERK (t-ERK1/2) or anti-phospho-ERK (p-ERK1/2) antibodies. In these studies, two sets of osteo-chondral explants were pre-treated with above inhibitors. They are designated as U.–1, SB.–1, U.–2, and SB.–2 on the blots, respectively.

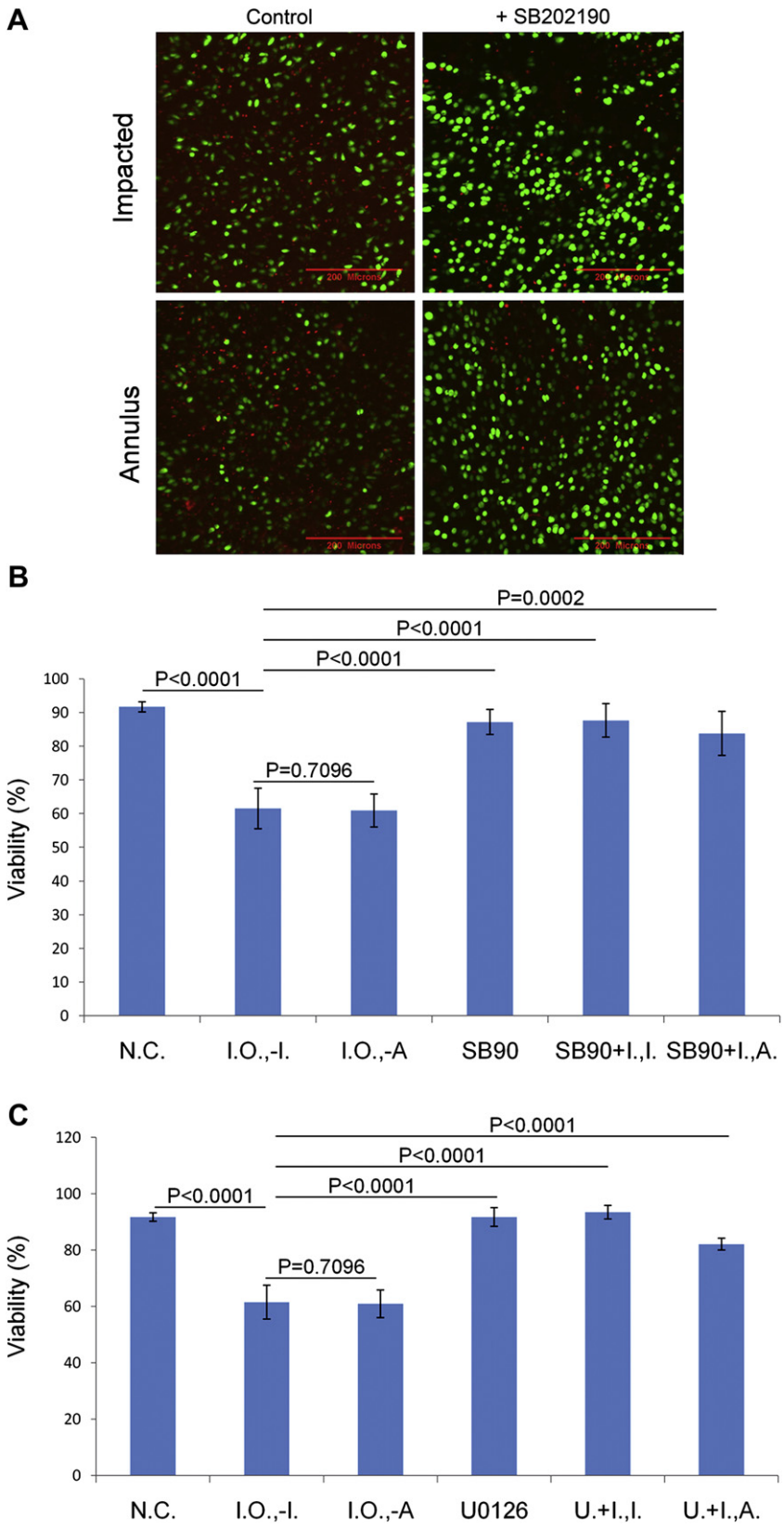

Fig. 6. Effects of MAP Kinase Inhibitors on Chondrocyte Viability after Impact Injury. (A) Confocal microscope images show impact and annulus sites on explants stained with calcein AM and ethidium homodimer on day 7 post-impaction. Green-stained cells are viable and red stained cell are dead. The explants shown in the panels on the right were treated with 10 μM p38 MAP kinase inhibitor (+SB202190). (B) The percentage of viable cells measured in non-impacted controls (N. C.), non-impacted controls treated with SB202190 only (SB90), impact sites in explants treated with SB202190 (SB90+I., −I.) or annulus sites in treated explants (SB90+I., −A.), and impact and annulus sites in untreated explants (Impact Only; I. O., −I.; I. O., −A.) ($N = 9$; Error bars stand for 95% CIs) (C) Percentage viability in non-impacted controls (N.C.), non-impacted controls treated with 10 μM ERK inhibitor, U0126, only (U0126) and impact and annulus sites treated with (U. + I., −I.; U. + I., −A.) or without UO126 (Impact Only; I. O., −I.; I. O., −A.) ($N = 9$; Error bars stand for 95% CIs). The viability of each group was compared to that of impact site from impacted explants without inhibitor treatment (Impact Only, I. O.).

SB202190 significantly increased cell viability in impact and annulus sites from 61.5% ± 6.01 and 60.9% ± 7.5 to 87.7% ± 4.97 ($P < 0.0001$) and 83.8% ± 6.53 ($P = 0.0002$), respectively. Those values were close to the percentages in non-impacted controls or cartilage treated with the inhibitor only [Fig. 6(B)]. Another p38 MAP kinase inhibitor, SB203580, also enhanced chondrocyte viability in impact and annulus sites but with less extent when compared to SB202190 (data not shown). Similar to p38 inhibitors, the MEK/ERK inhibitor, U0126, enhanced average live cell percentage in impact sites from 61.5% ± 6.01 to 93.4% ± 2.42 and in annulus sites from 60.9% ± 7.5 to 82.1% ± 2.09 respectively [Fig. 6 (C)]. This effect was statistically significant ($P < 0.0001$ for both the impact site and annulus site) and resulted in viable cell percentages similar to those in non-impacted cartilage or cartilage treated with the inhibitor only.

The effects of MAPK inhibitors on PG content in impact and annulus cartilage were measured at 7 days post-impaction and in non-impacted controls (Table I). The average PG content in impacted and annulus cartilage was 38.5 μg PG/mg wet cartilage and 45.9 μg PG/mg wet cartilage respectively, levels that were significantly lower than those in non-impacted cartilage (65.0 μg PG/mg), or cartilage treated with DMSO only (64.7 μg PG/mg). However, when the p38 MAPK inhibitor SB202190 was constantly present in the cultures, PG content increased to 75.2 μg PG/mg in impact sites and to 70.7 μg PG/mg in annulus sites, effects that were highly significant ($P = 0.0174$ for impact sites and $P = 0.0162$ for annulus sites). A second p38 inhibitor, SB203580, increased PG content from 38.5 μg PG/mg to 54.1 μg PG/mg in impact sites and from 45.9 μg PG/mg to 53.3 μg PG/mg in annulus sites. Although the increase in PG concentration was statistically significant in impact sites ($P = 0.0313$), SB203580 did not completely restore PG content to the level in non-impacted controls. U0126, an ERK pathway inhibitor, also significantly enhanced PG content, from 38.5 μg PG/mg to 71.5 μg PG/mg in the impact sites and from 45.9 μg PG/mg to 66.2 μg PG/mg in annulus sites. The PG levels in U0126 treated impacted cartilage were similar to that in non-impacted controls (65.0 μg PG/mg). The effects of U0126 on PG contents in both impact sites and annulus sites were statistically significant ($P = 0.0007$ for impact sites and $P = 0.0011$ for annulus sites).

Quantitative RT-PCR analysis of mRNA levels revealed significantly elevated expression of MMP-13, TNF-α and ADAMTS-5 in cartilage from the impacted zone and surrounding area at 6 h post-impaction (Table II). Compared to controls, impact zones showed increased expression of MMP-13 (2.6-fold, $P = 0.0394$), TNF-α (2.2-fold, $P = 0.0088$), and ADAMTS-5 (2.0-fold, $P = 0.0290$). Even higher relative expression of MMP-13 and TNF-α was detected in cartilage surrounding the impacted zone (3.1-fold and 2.9-fold respectively). These differences were statistically significant (For MMP-13: $P = 0.0158$; For TNF-α: $P = 0.0082$). Although the expression of ADAMTS-5 in the surrounding annulus cartilage was 1.6-fold higher than that in controls, the difference was not significant ($P = 0.1320$).

Table I
Effects of MAPK inhibitors on reducing blunt impact-induced PG depletion

Group	[PG] μg/mg wet cartilage		N	95% CIs		*P*
	Mean	S.D.		Upper limit	Lower limit	
Non-impacted control	65.0	2.65	3	68	62	0.0007
DMSO Only	64.7	7.51	3	73.2	56.2	0.0062
D. + I., −I.	38.5	4.17	3	43.22	33.78	N/A
D. + I., −A.	45.9	3.49	3	49.85	41.95	0.0779
Impact Only, −I.	47.4	8.14	3	56.61	38.19	0.1672
Impact Only, −A.	42.6	4.92	3	48.17	37.03	0.3327
SB203580 Only	57.2	4.33	3	62.1	52.3	0.0057
SB80 + I., −I.	54.1	7.18	3	62.22	45.98	0.0313
SB80 + I., −A.	53.3	8.37	3	62.77	43.83	0.0518
SB202190 Only	59.6	6.01	3	66.4	52.8	0.0075
SB90 + I., −I.	75.2	15.71	3	92.98	57.42	0.0174
SB90 + I., −A.	70.7	13.32	3	85.77	55.63	0.0162
U0126 only	54.2	9.56	3	65.02	43.38	0.0596
U. + I., −I.	71.5	4.49	3	76.58	66.42	0.0007
U. + I., −A.	66.2	3.83	3	70.53	61.87	0.0011

The PG contents in impacted cartilage or non-impacted controls were measured at Day 7of post-impaction. In impacted explants, cartilage directly from the impact zone (−I.) along with areas immediately adjacent to the zone (−A.) were assayed. All values were compared to that of the impact site of impacted cartilage treated with DMSO (D. + I., −I.).

Discussion

In-vitro studies show that mechanical trauma to articular cartilage causes immediate physical damage to the collagen network[30] and biologic responses that lead to increased ECM turnover[31,32], elevated cartilage degradation[33,34], and reduced cell viability[35–38]. Previously published data based on our *in vitro* injury model showed that the caspase inhibitor z-VAD-fmk saved approximately 30–50% of cells that otherwise died within 24 h of impaction[45]. This indicated that caspase-dependent apoptosis was responsible for 30–50% of blunt impaction-induced cell death. However, more work needs to be done in order to investigate the causes of cell death at different time points and at different energy levels of a single blunt impact on cartilage.

The early activation of p38 and JNK MAP kinases in impact and adjacent cartilage could be the direct result of mechanical force. Deformation of the ECM can be sensed by trans-membrane receptors, such as beta 1 integrins, which signal *via* MAP kinases[39]. The beta 1 integrin-p38 pathway was shown to mediate p53 activation and apoptosis of smooth muscle cells subjected to cyclic mechanical stretch[40]. Therefore, the early activation of p38 and JNK kinases in our model suggest apoptotic pathways might be turned on, which in turn induces cell death in both impact zone and in cartilage adjacent to the zone.

Cytokines or fragmented ECM components including fibronectin, collagen, and hyaluronic acid, might well be responsible for inducing the activation of p38 and ERK1/2 at later time points[22,41,42]. ERKs have been shown to mediate signaling to downstream kinases and transcription factors, resulting in increased expression of genes involved in cell proliferation and migration, which may be part of a reparative process[43]. On the other hand, ERKs modulate apoptotic pathways in chondrocytes

Table II
Up-regulation of catabolic genes by blunt impact

Group	$2^{-\Delta\Delta CT}$		N	95% CIs		*P*
	Mean	S.D.		Upper limit	Lower limit	
MMP-13						
Control	1	0.90	3	2.02	−0.02	N/A
Impact	2.57	0.03	3	2.6	2.54	0.0394
Annulus	3.11	0.11	3	3.23	2.99	0.0158
TNF-α						
Control	1	0.32	3	1.36	0.64	N/A
Impact	2.23	0.31	3	2.58	1.88	0.0088
Annulus	2.91	0.60	3	3.59	2.23	0.0082
ADMTS-5						
Control	1	0.52	3	1.59	0.41	N/A
Impact	2.01	0.07	3	2.09	1.93	0.0290
Annulus	1.60	0.18	3	1.8	1.4	0.1320

The mRNA levels of target genes in cartilage at 6 h of post-impaction were measured with quantitative real-time PCR. The relative expression of target genes was calculated as ratios of CT values in impacted or annulus cartilage to those in untreated control cartilage ($2^{-\Delta\Delta CT}$).

and have been shown to act synergistically with p38 MAP kinase to promote apoptosis[44]. The strong beneficial effects of the ERK inhibitor on viability in our model lend support to this hypothesis.

The results of this investigation confirmed sequential activation of p38 and ERK1/2 after blunt impact injury. The kinases were activated not just in cartilage damaged directly by impaction, but in the adjacent undamaged cartilage. Impact-related chondrocyte mortality and cartilage PG loss in both impacted and adjacent cartilage were inhibited by p38 and ERK inhibitors, indicating that these kinases play a role in initiating and propagating chondrolytic activity after mechanical injury. Since these results raised the possibility that p38 and ERK1/2 act in the same pathway, we studied the effect of p38 inhibition on ERK activation following impaction. The results clearly showed that ERK activation was not affected by blocking the p38 pathway. However, the two pathways might converge in the nucleus to act together on transcription factors that regulate catabolic and anabolic pathways and even cell death.

Although we observed that inhibiting p38 pathway or ERK pathway effectively reduced impaction-induced cell death and ECM depletion, our findings do not allow us to conclude if increased PG content associated with inhibitor treatments were due to reduced catabolic activity, increased anabolic activity, or simply to preservation of viability (or all three). In addition, sample-to-sample variation among the osteo-chondral explants used for this study might occasionally have led to increases in phospho/total ERK1/2 ratios that were not related to impaction. Nevertheless, densitometry data based on multiple blots showed that, in relation to total ERK1/2, phospho-ERK1/2 increased several fold by 24 h of post-impaction, a change that did not occur consistently in non-impacted controls.

The significantly elevated expression of MMP-13, TNF-α and ADAMTS-5 at 6 h post-impaction indicate that MAP kinase activation leads to overexpression of catabolic factors. This hypothesis is based on the observations that both p38 and ERK MAP kinases play important roles in up-regulating genes involved in cartilage degradation[22,46], mediating TNF-α induced suppression of type II collagen and link protein[47].

Previous work in our laboratory demonstrated that acute impact-induced cell death was substantially inhibited by immediate post-impact treatment (within 4 h) with n-acetyl cysteine (NAC), a free radical scavenger[45]. However, without any further intervention, the catabolic activities of surviving cells may still lead to progressive degeneration. In that regard, the complete blockade of PG depletion by the MAP kinase inhibitors tested in our model system suggests they may be useful as a follow-up treatment to NAC.

Our model is limited by the absence of synovium and other factors that govern cartilage responses in clinically-relevant joint injuries. Although we chose to focus here on the effects of impact injury itself, post-impaction static or cyclic loading might as well contribute to the propagation of ECM degradation by activating or strengthening multiple catabolic pathways. The long-term development of PTOA is impossible to predict based on events studied here, which spanned only the first 24 h of post-injury. Nevertheless, our study supports the concept that cartilage degeneration is not an inevitable consequence of mechanical injury and points to multiple pathways involved in impaction-induced cartilage degradation as promising targets for testing in *in vivo* models.

Author contributions

Conception and design: James Martin, Joseph Buckwalter, Lei Ding.

Analysis and interpretation: Lei Ding, James Martin, Gene Homandberg.

Drafting of the article: Lei Ding.

Critical revision: James Martin, Joseph Buckwalter.

Final approval: Joseph Buckwalter, James Martin.

Provision of study materials: Nicolas Stroud.

Statistical expertise: Lei Ding.

Obtaining of funding: Joseph Buckwalter, James Martin, Gene Homandberg.

Administrative, technical, or logistic support: Danping Guo.

Collection and assembly of data: Lei Ding, Emily Heying, Nathan Nicholson.

Role of the funding sources

This work was supported by a NIAMS grant (#1 P50 AR055533) and by a Merit Review Award from the Department of Veterans Affaires. The study sponsors have no involvement in the study design, collection, analysis and interpretation of data, in the writing of the manuscript, or in the decision to submit the manuscript for publication.

Conflict of interest

The authors declare they have no conflicts of interest.

Acknowledgements

Confocal microscopy was performed in the University of Iowa Central Microscopy Research Facility. We thank Barbara Laughlin, Abigail Lehman, Julie Amendola, Lois Lembke and Theresa Guither for technical assistance.

References

1. Buckwalter JA, Martin JA. Sports and osteoarthritis. Curr Opin Rheumatol 2004;16:634–9.
2. Buckwalter JA, Brown TD. Joint injury, repair, and remodeling: roles in post-traumatic osteoarthritis. Clin Orthop Relat Res 2004 Jun;(423):7–16.
3. Buckwalter JA, Martin JA, Mankin HJ. Synovial joint degeneration and the syndrome of osteoarthritis. Instr Course Lect 2000;49:481–9.
4. Jeffrey JE, Gregory DW, Aspden RM. Matrix damage and chondrocyte viability following a single impact load on articular cartilage. Arch Biochem Biophys 1995;322:87–96.
5. Sah RLY, Doong AJ, Grodzinsky AJ, Plaas AHK, Sandy JD. Effects of compression on the loss of newly-synthesised proteoglycans in cartilage explants. Arch Biochem Biophys 1991;286 (1):20–9.
6. Aigner T, McKenna L. Molecular pathology and pathobiology of osteoarthritic cartilage. Cell Mol Life Sci 2002;59(1):5–18.
7. Blanco FJ, Guitian R, Vazquez-Martul E, de Toro FJ, Galdo F. Osteoarthritis chondrocytes die by apoptosis. A possible pathway for osteoarthritis pathology. Arthritis Rheum 1998;41 (2):284–9.
8. Hashimoto S, Ochs RL, Komiya S, Lotz M. Linkage of chondrocyte apoptosis and cartilage degradation in human osteoarthritis. Arthritis Rheum 1998;41(9):1632–8.
9. Hashimoto S, Ochs RL, Rosen F, Quach J, McCabe G, Solan J, *et al*. Chondrocyte-derived apoptotic bodies and calcification of articular cartilage. Proc Natl Acad Sci U S A 1998;95 (6):3094–9.
10. Martin JA, Buckwalter JA. Post-traumatic osteoarthritis: the role of stress induced chondrocyte damage. Biorheology 2006;43(3–4):517–21.
11. D'Lima DD, Hashimoto S, Chen PC, Colwell Jr CW, Lotz MK. Human chondrocyte apoptosis in response to mechanical injury. Osteoarthritis Cartilage 2001;9(8):712–9.

12. Costouros JG, Dang AC, Kim HT. Comparison of chondrocyte apoptosis in vivo and in vitro following acute osteochondral injury. J Orthop Res 2004;22(3):678–83.
13. Hembree WC, Ward BD, Furman BD, Zura RD, Nichols LA, Guilak F, *et al*. Viability and apoptosis of human chondrocytes in osteochondral fragments following joint trauma. J Bone Joint Surg Br. 2007 Oct;89(10):1388–95.
14. Ficat C. The reaction of articular cartilage to mechanical trauma. An experimental study. Rev Chir Orthop Reparatrice Appar Mot 1976 Jul–Aug;62(5):493–500.
15. Roach HI, Aigner T, Kouri JB. Chondroptosis: a variant of apoptotic cell death in chondrocytes? Apoptosis 2004;9(3):265–77.
16. Kurz B, Lemke AK, Fay J, Pufe T, Grodzinsky AJ, Schünke M. Pathomechanisms of cartilage destruction by mechanical injury. Ann Anat 2005 Nov;187(5–6):473–85.
17. Borrelli Jr J, Tinsley K, Ricci WM, Burns M, Karl IE, Hotchkiss R. Induction of chondrocyte apoptosis following impact load. J Orthop Trauma 2003 Oct;17(9):635–41.
18. Tew SR, Kwan AP, Hann A, Thomson BM, Archer CW. The reactions of articular cartilage to experimental wounding: role of apoptosis. Arthritis Rheum 2000;43(1):215–25.
19. Chen CT, Burton-Wurster N, Borden C, Hueffer K, Bloom SE, Lust G. Chondrocyte necrosis and apoptosis in impact damaged articular cartilage. J Orthop Res 2001;19(4):703–11.
20. Sofat N. Analysing the role of endogenous matrix molecules in the development of osteoarthritis. Int J Exp Pathol 2009 Oct;90 (5):463–79.
21. Chowdhury TT, Salter DM, Bader DL, Lee DA. Signal transduction pathways involving p38 MAPK, JNK, NFkappaB and AP-1 influences the response of chondrocytes cultured in agarose constructs to IL-1beta and dynamic compression. Inflamm Res. 2008 Jul;57(7):306–13.
22. Ding L, Guo D, Homandberg GA. The cartilage chondrolytic mechanism of fibronectin fragments involves MAP kinases: comparison of three fragments and native fibronectin. Osteoarthritis Cartilage 2008 Oct;16(10):1253–62.
23. Ruettger A, Schueler S, Mollenhauer JA, Wiederanders B. Cathepsins B, K, and L are regulated by a defined collagen type II peptide via activation of classical protein kinase C and p38 MAP kinase in articular chondrocytes. J Biol Chem. 2008 Jan 11;283(2):1043–51.
24. Guo D, Ding L, Homandberg GA. Telopeptides of type II collagen upregulate proteinases and damage cartilage but are less effective than highly active fibronectin fragments. Inflamm Res. 2009 Mar;58(3):161–9.
25. Im JS, Lee JK. ATR-dependent activation of p38 MAP kinase is responsible for apoptotic cell death in cells depleted of Cdc7. J Biol Chem 2008 Sep 12;283(37):25171–7.
26. Tan H, Ling H, He J, Yi L, Zhou J, Lin M, *et al*. Inhibition of ERK and activation of p38 are involved in diallyl disulfide induced apoptosis of leukemia HL-60 cells. Arch Pharm Res. 2008 Jun;31(6):786–93.
27. Liu WH, Cheng YC, Chang LS. ROS-mediated p38alpha MAPK activation and ERK inactivation responsible for upregulation of Fas and FasL and autocrine Fas-mediated cell death in Taiwan cobra phospholipase A(2)-treated U937 cells. J Cell Physiol 2009 Jun;219(3):642–51.
28. Lee S, Lee M, Kim SH. Eupatilin inhibits H(2)O(2)-induced apoptotic cell death through inhibition of mitogen-activated protein kinases and nuclear factor-kappaB. Food Chem Toxicol 2008 Aug;46(8):2865–70.
29. Pelletier JP, Fernandes JC, Jovanovic DV, Reboul P, Martel-Pelletier J. Chondrocyte death in experimental osteoarthritis is mediated by MEK 1/2 and p38 pathways: role of cyclooxygenase-2 and inducible nitric oxide synthase. J Rheumatol 2001 Nov;28(11):2509–19.
30. Wilson W, van Burken C, van Donkelaar C, Buma P, van Rietbergen B, Huiskes R. Causes of mechanically induced collagen damage in articular cartilage. J Orthop Res. 2006 Feb;24(2):220–8.
31. Quinn TM, Grodzinsky AJ, Buschmann MD, Kim YJ, Hunziker EB. Mechanical compression alters proteoglycan deposition and matrix deformation around individual cells in cartilage explants. J Cell Sci. 1998 Mar;111(Pt 5):573–83.
32. Quinn TM, Grodzinsky AJ, Hunziker EB, Sandy JD. Effects of injurious compression on matrix turnover around individual cells in calf articular cartilage explants. J Orthop Res. 1998 Jul;16(4):490–9.
33. Davis MA, Ettinger WH, Neuhaus JM, Cho SA, Hauck WW. The association of knee injury and obesity with unilateral and bilateral osteoarthritis of the knee. Am J Epidemiol 1989;130: 278–88.
34. Howell DS, Treadwell BV, Trippel SB. Etiopathogenesis of osteoarthritis. In: Moskowitz RW, Howell DS, Goldberg VM, Eds. Osteoarthritis: diagnosis and medical/surgical management. 2nd edn. Philadelphia: W.B. Saunders; 1992:233–52.
35. Repo RU, Finlay JB. Survival of articular cartilage after controlled impact. J Bone Joint Surg 1977;59:1068–76.
36. Torzilli PA, Grigiene R, Borrelli J, Helfet DL. Effect of impact load on articular cartilage: cell metabolism and viability and matrix water content. J Biomech Eng 1999;121:433–41.
37. Walker EA, Verner A, Flannery CR, Archer CW. Cellular responses of embryonic hyaline cartilage to experimental wounding in vitro. J Orthop Res 2000;18:25–34.
38. Green DM, Noble PC, Ahuero JS, Birdsall HH. Cellular events leading to chondrocyte death after cartilage impact injury. Arthritis Rheum 2006 May;54(5):1509–17.
39. Lal H, Verma SK, Smith M, Guleria RS, Lu G, Foster DM, *et al*. Stretch-induced MAP kinase activation in cardiac myocytes: differential regulation through beta1-integrin and focal adhesion kinase. J Mol Cell Cardiol 2007 Aug;43(2):137–47.
40. Wernig F, Mayr M, Xu Q. Mechanical stretch-induced apoptosis in smooth muscle cells is mediated by beta1-integrin signaling pathways. Hypertension 2003 Apr;41(4):903–11.
41. Homandberg GA, Ding L, Guo DP. Extracellular matrix fragments as regulators of cartilage metabolism in health and disease. Curr Rheumatol Rev August 2007;3(3):183–96 (14).
42. Homandberg GA, Ding L, Guo DPIn: The role of extracellular matrix fragments in the autocrine regulation of cartilage metabolism. Osteoarthritis, inflammation and degradation: a continuum. Biomedical and Health Research; 2007;Vol. 70
43. Ryan JA, Eisner EA, DuRaine G, You Z, Reddi AH. Mechanical compression of articular cartilage induces chondrocyte proliferation and inhibits proteoglycan synthesis by activation of the ERK pathway: implications for tissue engineering and regenerative medicine. J Tissue Eng Regen Med 2009 Feb;3(2):107–16.
44. Berenbaum F, Humbert L, Bereziat G, Thirion S. Concomitant recruitment of ERK1/2 and p38 MAPK signalling pathway is required for activation of cytoplasmic phospholipase A2 via ATP in articular chondrocytes. J Biol Chem. 2003 Apr 18;278 (16):13680–7.
45. Martin JA, McCabe D, Walter M, Buckwalter JA, McKinley TO. N-acetylcysteine inhibits post-impact chondrocyte death in osteochondral explants. J Bone Joint Surg Am 2009;91:1890–7.
46. Echtermeyer F, Bertrand J, Dreier R, Meinecke I, Neugebauer K, Fuerst M, *et al*. Syndecan-4 regulates ADAMTS-5 activation and cartilage breakdown in osteoarthritis. Nat Med 2009 Sep;15 (9):1072–6.
47. Séguin CA, Bernier SM. TNFalpha suppresses link protein and type II collagen expression in chondrocytes: role of MEK1/2 and NF-kappaB signaling pathways. J Cell Physiol 2003 Dec;197(3):356–69.